

Supplement to November / December 2021

Volume 50, Number 6

Applied Radiology®

50
YEARS

The Journal of Practical Medical Imaging and Management

Celebrating Our Pediatric Community



Choledochoceles

Congenital
Diaphragmatic
Hernia

Congenital Venous
Malformation

Telangiectatic
Osteosarcoma

Middle Aortic Syndrome

Sponsored by

Guerbet | 

Applied Radiology®

The Journal of Practical Medical
Imaging and Management

Anderson Publishing, Ltd
180 Glenside Avenue,
Scotch Plains, NJ 07076
Tel: 908-301-1995
Fax: 908-301-1997
info@appliedradiology.com

PRESIDENT & CEO

Oliver Anderson

GROUP PUBLISHER

Kieran N Anderson

ASSOCIATE PUBLISHER

Cristine Funke, RT(R)

EDITOR-IN-CHIEF

Erin Simon Schwartz, MD, FACR

EXECUTIVE EDITOR

Joseph F Jalkiewicz

PRODUCTION

Barbara A Shopiro

Contents

4 Choledochoceles

Alec R Smith, Richard B Towbin, MD; Yinan Li, MD; David S Vitale, MD;
Alexander J Towbin, MD

8 Congenital Diaphragmatic Hernia

Joy E Lee, Richard B Towbin, MD; David J Aria, MD; Carrie M Schaefer, MD;
Alexander J Towbin, MD

11 Congenital Venous Malformation

Diep Nguyen, Richard B Towbin, MD; Carrie M Schaefer, MD; Alexander J
Towbin, MD; David J Aria, MD

18 Telangiectatic Osteosarcoma

Colby S Nielsen; Richard B Towbin, MD; Carrie M Schaefer, MD; Alexander J
Towbin, MD; David J Aria, MD

21 Middle Aortic Syndrome

Kenneth Zurcher, MD; Richard B Towbin, MD; Carrie M. Schaefer; Scott A
Jorgensen, MD; Alexander J Towbin, MD

The Pediatric Community Comes of Age

Richard B Towbin, MD, and Alexander J Towbin, MD

It was in late 2014 that we approached Kieran Anderson, publisher of *Applied Radiology*, about helping us to create an online community for students, residents, fellows, and staff radiologists with an interest or specialization in pediatric radiology.

Our goal, we explained to Kieran, was to publish material highlighting the breadth and depth of our specialty for medical professionals at all stages of their career. We shared our vision for a place for all to share interesting cases and other material related to this amazing sub-specialty of medical imaging.

Kieran signed on, and *Applied Radiology's* online Pediatric Community was born.

Seven years on, we have published some 70 case reports, papers, and how-to procedural guides focusing on pediatric radiology. At first, most of these were written by faculty and fellows. Eventually, medical students began appearing as first authors on a growing number of articles. To date, 30 medical students have been published in the Pediatric Community, reflecting our singular focus on fostering interest and excitement in pediatric radiology among students and residents in medical and surgical subspecialties. The Community has earned the

sponsorship of Guerbet and now boasts 4,500 visits each month.

They say imitation is the sincerest form of flattery; perhaps one of the best measures of our success is in seeing others duplicate our efforts. In addition to the Pediatric Community, *Applied Radiology* now hosts several other new communities for breast imaging, computed tomography, magnetic resonance, vascular and interventional radiology, and artificial intelligence.

We believe the Pediatric Community is well positioned to support trainees well into the future. Indeed, we have plans to increase the number of papers we publish, provide inexpensive CME credits, develop opinion pieces, host more webinars, and more.

In closing, let us just say we have been blown away by the success of the Pediatric Community. Please know that our mission is and always will be to provide you with a place of your own to share and learn what's new in pediatric radiology.

Thank you for the opportunity to serve, and we look forward to your continued support in the years ahead.

Respectfully,
Richard B Towbin, MD
Alexander J Towbin, MD

Choledochoceles

Alec R Smith, Richard B Towbin, MD; Yinan Li, MD; David S Vitale, MD; Alexander J Towbin, MD

Case Summary

Abdominal imaging was performed to evaluate for distant disease in a child with scalp melanoma. A choledochocoele was found incidentally during imaging evaluation. At that time, the child had no abdominal pain, jaundice, or hematemesis and did not exhibit signs of hepatic injury or cholestasis.

The patient was lost to follow-up for four years and presented again for re-evaluation. Magnetic resonance imaging (MRI) showed enlargement of the choledochocoele. They again had no symptoms of abdominal pain, difficulty eating, or jaundice, but the child's mother noted occasional, bright, green-colored stools. Liver function tests demonstrated mild elevation of AST and ALT but no cholestasis. The patient and her family elected for management of the choledochocoele with an endoscopic retrograde cholangiopancreatography (ERCP) with endoscopic biliary sphincterotomy and biopsy of the cyst lining.

Imaging Findings

The initial MRI (Figure 1) identified a mildly enlarged common bile duct (CBD) (5 mm diameter) with mild central intrahepatic biliary ductal dilatation. The dilated CBD inserted into a bilobed cystic structure at the level of the pancreatic head. One lobe of this structure appeared partially intraluminal, extending into the second portion of the duodenum and was diagnosed as a choledochocoele. The hepatobiliary phase images showed the cystic structure filling with contrast.

Follow-up magnetic resonance cholangiopancreatography (MRCP, Figure 2) four years later showed similar prominence of the central confluence of the hepatic ducts. The CBD remained dilated, measuring 7 mm in diameter and tapering to a point at the level of the ampulla. The choledochocoele was again seen protruding into the duodenal lumen. The pancreatic duct was normal in caliber.

An ERCP confirmed the diagnosis of a Type III choledochal cyst — a choledochocoele (Figure 3). A cholangiogram showed a dilated main bile duct with mildly dilated intrahepatic ducts. A needle knife cystostomy followed by sphincterotomy extension of the

cystostomy and biliary sphincterotomy was performed.

Diagnosis

Choledochocoele (Type III choledochal cyst).

The differential diagnosis includes duodenal duplication cyst, other types of choledochal cysts, pancreatic pseudocyst, impacted gallstone, and biliary stricture.

Discussion

Choledochal cysts are dilations in the biliary tree. The Todani classification system defines six types of choledochal cysts, depending on the location of dilation. Type III choledochal cysts are limited to the intraduodenal portion of the CBD. These cysts are recognized as congenital anomalies and are more commonly known as choledochoceles, a term first applied in 1940, owing to their similarity to ureterocele.² There are two subtypes of choledochoceles, A and B.^{2,3} Type A choledochoceles are characterized by both the pancreatic duct and CBD opening into the cystic space, which then communicates with the duodenum via a separate orifice.^{3,6} Type B choledochoceles occur when a diverticulum arises from

Affiliations: University of Arizona College of Medicine-Phoenix (Mr Smith); Phoenix Children's Hospital, Phoenix, AZ (Dr R Towbin); Cincinnati Children's Hospital and University of Cincinnati College of Medicine (Drs Li, Vitale, A Towbin).

Figure 1. (A) Coronal maximum intensity projection image from an MRCP shows a small cystic structure (arrow) arising from the insertion of the common bile duct at the ampulla of Vater. The thin rim of the cyst wall is seen at the periphery of the cyst. The normal pancreatic duct (arrowhead) joins with the common bile duct near the ampulla. (B) Postcontrast T1 image obtained in the hepatobiliary phase after administration of a hepatocyte-specific contrast agent shows contrast filling the common bile duct and cystic structure (arrow).

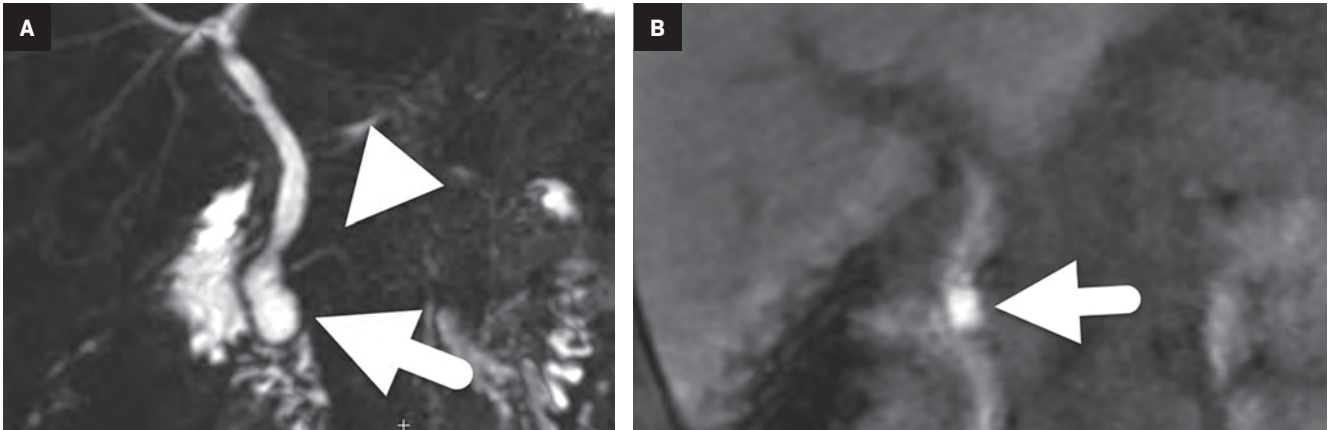


Figure 2. Coronal T2 MRI performed five years later shows the cystocele (arrow) extending into the duodenal lumen. The common bile duct is dilated..



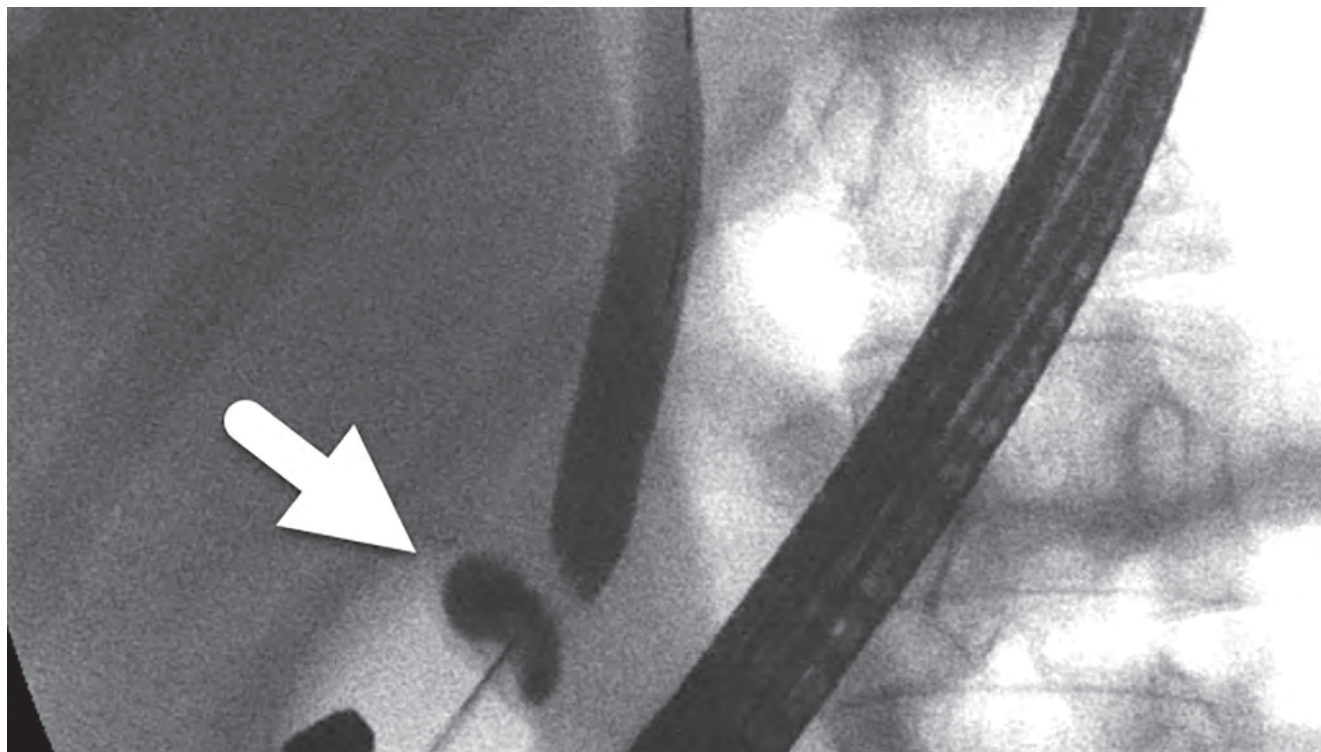
the intra-ampullary pancreaticobiliary duct or from the intraduodenal CBD. The bile and pancreatic secretions then drain into the duodenum via the ampulla of Vater.^{6,8} In both subtypes, the dilation can be visualized during endoscopic evaluation as an intraduodenal bulge at the

level of the major duodenal papilla.

Choledochoceles are rare, making up fewer than 5% of choledochal cysts, and are more commonly diagnosed in adults than children.^{1,2,3,5} Choledochoceles differ from other choledochal cysts in that they affect males and

females equally (other choledochal cysts have a well-established 3:1 female to male ratio).^{1,3,5} Patients with a prior biliary procedure are thought to have a higher risk of acquiring a choledochoceles. This is supported by the literature, which reports prior cholecystectomy or

Figure 3. ERCP image shows the cystocele (arrow) at the luminal aspect of the dilated common bile duct.



CBD exploration in 44-60% of adult patients with choledochoceles.^{2,7} In children, these are generally considered congenital abnormalities.

Various theories have been put forth to explain the etiology of choledochal cysts. The prevailing theory is that an anomalous pancreaticobiliary junction (APBJ) leads to pancreaticobiliary reflux, which ultimately causes inflammation, cystic dilation, and an increased risk for malignancy.⁸ However, an APBJ is not found in all patients with choledochoceles.² Other congenital etiologies include failed regression of a rudimentary CBD during embryological development or a congenital intramural cyst or diverticulum.^{1,3,5,6} Evidence supporting a congenital etiology of choledochoceles includes the presence of duodenal mucosa in nearly two-thirds of cysts.^{2,3} An acquired choledochocoele may result from any situation that causes inflam-

mation and chronically elevated pressure within the ampulla of Vater, with resulting obstructive intramural dilation of the CBD.^{1,2,3,6}

Patients with a choledochocoele most commonly present with abdominal pain, jaundice, nausea, vomiting, or a palpable mass.² These entities can also be encountered incidentally on imaging performed for unrelated indications, as in this patient. In contrast to patients with other types of choledochal cysts, those with a choledochocoele are more likely to present with acute pancreatitis and less likely to develop biliary tract symptoms and cholangitis.^{2,3,4}

Ultrasound is often the first-line imaging modality for patients presenting with signs and symptoms of an acute or subacute biliary abnormality. In patients with a choledochocoele, ultrasound can identify the intraduodenal cystic mass.^{2,3} Additionally, it can help to

determine the extent of a pancreaticobiliary abnormality and the presence or absence of intraductal biliary stones. MRCP is considered the noninvasive test of choice as it provides detailed anatomic information and helps to assess size, location, and nature of the cystic mass. ERCP is considered the diagnostic gold-standard, but it is an invasive intervention with associated risk factors.^{2,3} Currently, the major role of ERCP is to confirm the MRCP findings and to guide cystostomy and biliary sphincterostomy.^{2,3}

Studies report a risk of malignancy around 2.5%.^{1,3,4,5} In contrast, the risk of cancer with other choledochal cysts has been reported to range from 10-15%.^{1,2,4} It is surmised that the lower risk of malignancy is related to choledochoceles etiology. Because an APBJ is not routinely found in patients with a choledochocoele, the risk of reflux

and resulting cancer is thought to be decreased. An intraoperative biopsy is performed to help determine malignancy risk.

The lining of a choledochocoele can be either intestinal or biliary epithelium.⁷ Some researchers hypothesize that cysts lined with intestinal epithelium do not carry an increased risk of malignancy, while cysts lined with biliary epithelium may carry an increased risk of developing cholangiocarcinoma.

Treatment depends on malignancy risk and size of the choledochocoele.⁵ Endoscopic sphincterotomy and/or surgical marsupialization have been used if intestinal epithelium is present.^{5,7,11} Endoscopic sphincterotomy with cystotomy is the most widely used option; the procedure relieves any biliary obstruction and allows for cyst drainage. Endoscopic sphincterotomy outcomes are favorable, with quick, postsurgical resolution of symptoms.^{2,3} Alternatively, transmural excision of the choledochocoele is required if biliary or dysplastic epithelium is found or if the cyst is causing gastric outlet obstruction.^{4,5}

Conclusion

Choledochoceles are rare abnormalities of the biliary tree, with an etiology that is not well understood. Imaging often detects a cystic mass in the descending duodenum, and MRCP elucidates the anatomy and confirms the diagnosis. Choledochoceles affect adults most often, with no male or female preference.

Symptomatic patients present with abdominal pain, jaundice, and/or nausea/vomiting. Treatment consists most commonly of endoscopic sphincterotomy and cystotomy. Surgical excision may be necessary if there are findings of gastric outlet obstruction or dysplasia.

References

- 1) Singham J, Yoshida EM, Scudamore CH. Choledochal cysts: part 1 of 3: classification and pathogenesis. *Can J Surg*. 2009;52(5):434-440.
- 2) Ziegler KM, Zyromski NJ. Choledochoceles: are they choledochal cysts? *Adv Surg*. 2011;45:211-224. doi:10.1016/j.yasu.2011.03.019
- 3) Law R, Topazian M. Diagnosis and treatment of choledochoceles. *Clin Gastroenterol Hepatol*. 2014;12(2):196-203. doi:10.1016/j.cgh.2013.04.037
- 4) Soares KC, Arnaoutakis DJ, Kamel I, et al. Choledochal cysts: presentation, clinical differentiation, and management. *J Am Coll Surg*. 2014;219(6):1167-1180. doi:10.1016/j.jamcollsurg.2014.04.023
- 5) Lobeck IN, Dupree P, Falcone RA Jr, et al. The presentation and management of choledochocoele (type III choledochal cyst): A 40-year systematic review of the literature. *J Pediatr Surg*. 2017;52(4):644-649. doi:10.1016/j.jpedsurg.2016.10.008
- 6) Scholz FJ, Carrera GF, Larsen CR. The choledochocoele: correlation of radiological, clinical and pathological findings. *Radiology*. 1976;118(1):25-28. doi:10.1148/118.1.25
- 7) Schimpl G, Sauer H, Goriup U, Becker H. Choledochocoele: importance of histological evaluation. *J Pediatr Surg*. 1993;28(12):1562-1565. doi:10.1016/0022-3468(93)90097-5
- 8) Cha SW, Park MS, Kim KW, et al. Choledochal cyst and anomalous pancreatobiliary ductal union in adults: radiological spectrum and complications [published correction appears in *J Comput Assist Tomogr*. 2008 Sep-Oct;32(5):827]. *J Comput Assist Tomogr*. 2008;32(1):17-22. doi:10.1097/RCT.0b013e318064e723
- 9) Kamisawa T, Tu Y, Nakajima H, Egawa N, Tsuruta K, Okamoto A. The presence of a common channel and associated pancreaticobiliary diseases: a prospective ERCP study. *Dig Liver Dis*. 2007;39(2):173-179. doi:10.1016/j.dld.2006.09.020
- 10) Matsushita M, Uchida K, Nishio A, Okazaki K. Differential diagnosis of intraduodenal cystic lesions: choledochocoele, duodenal duplication cyst, or intraluminal duodenal diverticulum? *Gastrointest Endosc*. 2010;71(1):219-220. doi:10.1016/j.gie.2009.04.032
- 11) Lobeck IN, Dupree P, Falcone RA Jr, Lin TK, Trout AT, Nathan JD, Tiao GM. The presentation and management of choledochocoele (type III choledochal cyst): A 40-year systematic review of the literature. *J Pediatr Surg*. 2017;52(4):644-649. doi:10.1016/j.jpedsurg.2016.10.008

Congenital Diaphragmatic Hernia

Joy E Lee, Richard B Towbin, MD; David J Aria, MD; Carrie M Schaefer, MD; Alexander J Towbin, MD

Case Summary

A neonate presented with diminished breath sounds in the left chest. The infant's mother did not receive prenatal care.

Imaging Findings

The initial chest radiograph (Figure 1) showed herniated loops of bowel in the left hemithorax. The herniated contents caused mass effect, shifting the heart and mediastinum from left to right. The left hemidiaphragm was not visible. They underwent repair with a good postoperative result (Figure 2).

Diagnosis

Congenital diaphragmatic hernia (CDH).

The differential diagnosis for bubbly lucencies in the neonatal chest includes congenital pulmonary airway malformation, loculated pneumothorax or pneumomediastinum, and pleuropulmonary blastoma.^{1,2}

Discussion

Congenital diaphragmatic hernia is an anomaly that occurs in 2.3-2.8 per 10,000 births.³ The condition is associated with a variable diaphragmatic defect ranging from diaphragmatic thinning to complete absence of the hemidiaphragm.³ Lung development is often affected, and patients with CDH may have pulmonary hypoplasia and associated pulmonary hypertension.³

Classically, a CDH is a Bochdalek-type hernia, most commonly occurring in the posterolateral diaphragm (70%) and on the left side (85%).¹ It occurs because of inadequate closure of the posterior pleuroperitoneal membrane.³

CDH is usually diagnosed prenatally on a second- or third-trimester ultrasound. The diagnosis relies on observing abdominal contents within the chest and seeing the fluid-filled stomach posterior to the heart in the four-chamber view.¹ While most cases are diagnosed via prenatal ultrasound, up to 11% are diagnosed postnatally.¹

Fetal magnetic resonance imaging (MRI) allows radiologists to calculate morphometric features and provide useful prognostic information in the setting of CDH. Fetal lung volumes are the most

important predictor of long-term survival.¹ The prenatal observed/expected lung-to-head ratio is used for prognostic information and to select patients for fetal therapy.⁸ An observed/expected ratio < 25% indicates severe lung hypoplasia, while ratios of 25-35% indicate moderate hypoplasia.⁸ Fetuses with an observed/expected lung-to-head ratio between 25% and 35% have a 50-60% chance of survival.⁸

Postnatally, CDH patients may present with a barrel-shaped chest, absence of breath sounds on the affected side, a scaphoid abdomen, shifted cardiac sounds, and bowel sounds in the chest.⁴

Chest and abdominal radiographs often show an opacified hemithorax in the immediate postnatal period before distal bowel gas is present. As bowel gas progresses distally, bubbly lucencies fill loops of bowel. The herniated abdominal contents cause contralateral shift of the heart and mediastinum.⁵ Cross-sectional imaging may be used to more clearly visualize the associated anatomical defects in cases of suspected CDH and help to confirm the diagnosis.⁵

Whether the pulmonary hypoplasia associated with CDH stems from the diaphragmatic defect or an underlying issue with pulmonary

Affiliations: University of Arizona College of Medicine-Phoenix (Ms Lee); Phoenix Children's Hospital (Drs R Towbin, Aria, Schaefer); Cincinnati Children's Hospital (Dr A Towbin).

Figure 1. Radiograph of the chest and upper abdomen shows gas-filled structures within the left hemithorax that cause left-to-right shift of the heart and mediastinum. Some of gas-containing structures are amorphous in shape, while others look like colon with haustral markings (*). The abdomen is gasless. There is a malpositioned umbilical venous catheter in the left upper quadrant of the abdomen.

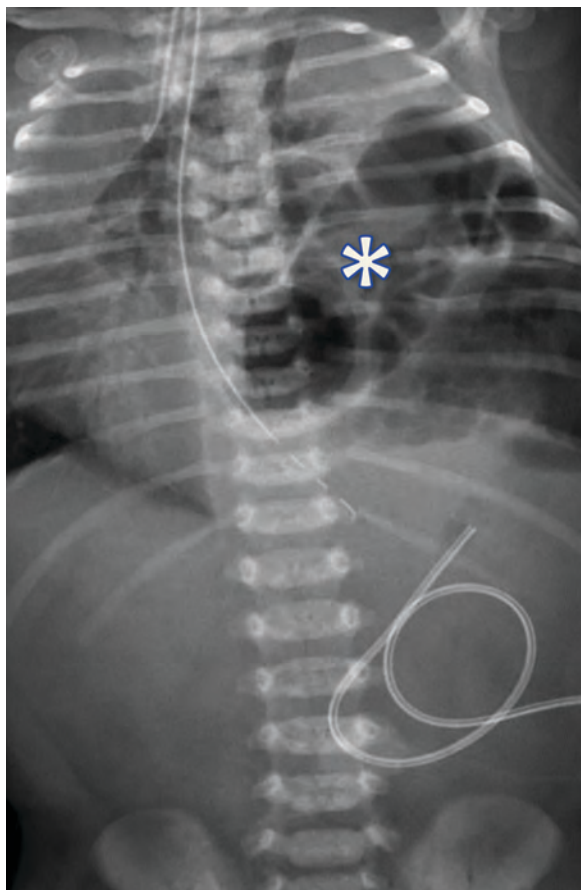
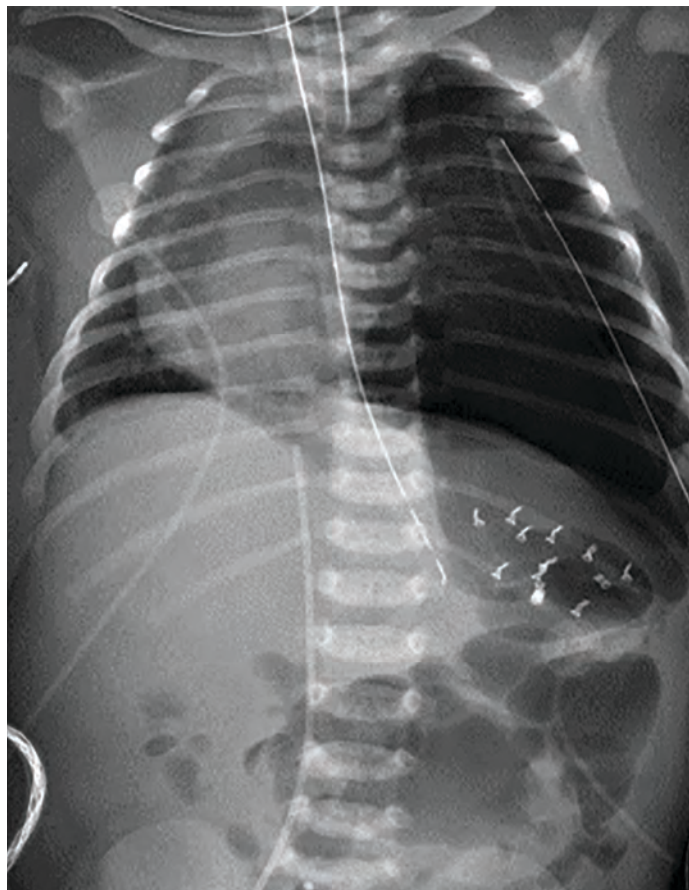


Figure 2. Follow-up chest radiograph shows the postoperative changes of the left hemidiaphragm, dextrocardia, or cardiac rotation secondary to the CDH, and a left-sided chest tube



development is unknown, but a “dual-hit” hypothesis based on animal models has been proposed.⁶ Although the underlying cause of pulmonary hypoplasia is poorly understood, upward-herniating abdominal contents in CDH are known to compress the ipsilateral lung, affecting terminal bronchiole, alveoli, and pulmonary vascular development.⁴ Additionally, a diaphragmatic defect causes a loss of negative pressure in the intrathoracic cavity, affecting lung development.⁵

Recent studies have sought to stratify CDH patients based on

mortality risk. Features such as a very low birth weight, low 5-minute Apgar score, cardiac or chromosomal anomalies, and supra-systemic pulmonary hypertension help to separate patients into low (10%), intermediate (20%), or high (50%) risk of mortality before discharge from the neonatal intensive care unit.⁹

Several different *in utero* approaches have been used to treat CDH in an attempt to promote lung growth. One of the most promising is fetal endoscopic tracheal occlusion (FETO).⁷ By occluding the trachea with a balloon from about 26 weeks to 34 weeks of gestation,

FETO causes a local increase in volume of fetal lung fluid which, in turn, causes lung growth.⁷

Infants with CDH are intubated and managed medically in preparation for corrective surgery.⁶ Typically, surgery is delayed until the neonate is physiologically stable, usually within a week of delivery.⁴ Management includes treatment of accompanying medical issues such as pulmonary hypertension, a major cause of mortality in these patients. In those with severe CDH, additional therapies such as ECMO may be utilized to help provide oxygen to the end-organs.⁴ Once the

patient is stable, the CDH may be surgically closed through primary or patch repair using an open or minimally invasive technique.⁴ Current data suggests that open surgical repair may lead to fewer postoperative complications.⁴

Patients treated for a CDH are at increased risk for long-term development of pulmonary disease related to pulmonary hypertension and pulmonary hypoplasia. Other long-term effects include gastrointestinal reflux, poor growth, neurodevelopmental delay and behavioral disorders, sensorineural hearing loss, and chest wall deformities.⁴

Conclusion

Congenital diaphragmatic hernia is a developmental defect often

detected prenatally, with clinical symptoms presenting soon after birth. Imaging plays a key role in the diagnosis of CDH. In this case, CDH was diagnosed postnatally upon presenting with diminished left-chest breath sounds, and successfully repaired with surgery.

References

- 1) Marlow J, Thomas J. A review of congenital diaphragmatic hernia. *Australas J Ultrasound Med.* 2013;16(1):16-21.
- 2) Zobel M, Gologorsky R, Lee H, Vu L. Congenital lung lesions. *Semin Pediatr Surg.* 2019;28(4):150821.
- 3) Gaxiola A, Varon J, Valladolid G. Congenital diaphragmatic hernia: an overview of the etiology and current management. *Acta Paediatr.* 2009;98(4):621-627.
- 4) Leeuwen L, Fitzgerald DA. Congenital diaphragmatic hernia. *J Paediatr Child Health.* 2014;50(9):667-673.
- 5) Taylor GA, Atalabi OM, Estroff JA. Imaging of congenital diaphragmatic hernias. *Pediatr Radiol.* 2009;39(1):1-16.
- 6) Keijzer R, Liu J, Deimling J, Tibboel D, Post M. Dual-hit hypothesis explains pulmonary hypoplasia in the nitrofen model of congenital diaphragmatic hernia. *Am J Pathol.* 2000;156(4):1299-1306.
- 7) Kardon G, Ackerman KG, McCulley DJ, et al. Congenital diaphragmatic hernias: from genes to mechanisms to therapies. *Dis Model Mech.* 2017;10(8):955-970. doi:10.1242/dmm.028365
- 8) Cordier AG, Russo FM, Deprest J, Benachi A. Prenatal diagnosis, imaging, and prognosis in Congenital Diaphragmatic Hernia. *Semin Perinatol.* 2020;44(1):51163.
- 9) Brindle ME, Cook EF, Tibboel D, Lally PA, Lally KP, Group CDHS. A clinical prediction rule for the severity of congenital diaphragmatic hernias in newborns. *Pediatrics.* 2014;134(2):e413-419.

Congenital Venous Malformation

Diep Nguyen, Richard Towbin, MD; Carrie M Schaefer, MD; Alexander J Towbin, MD; David J Aria, MD

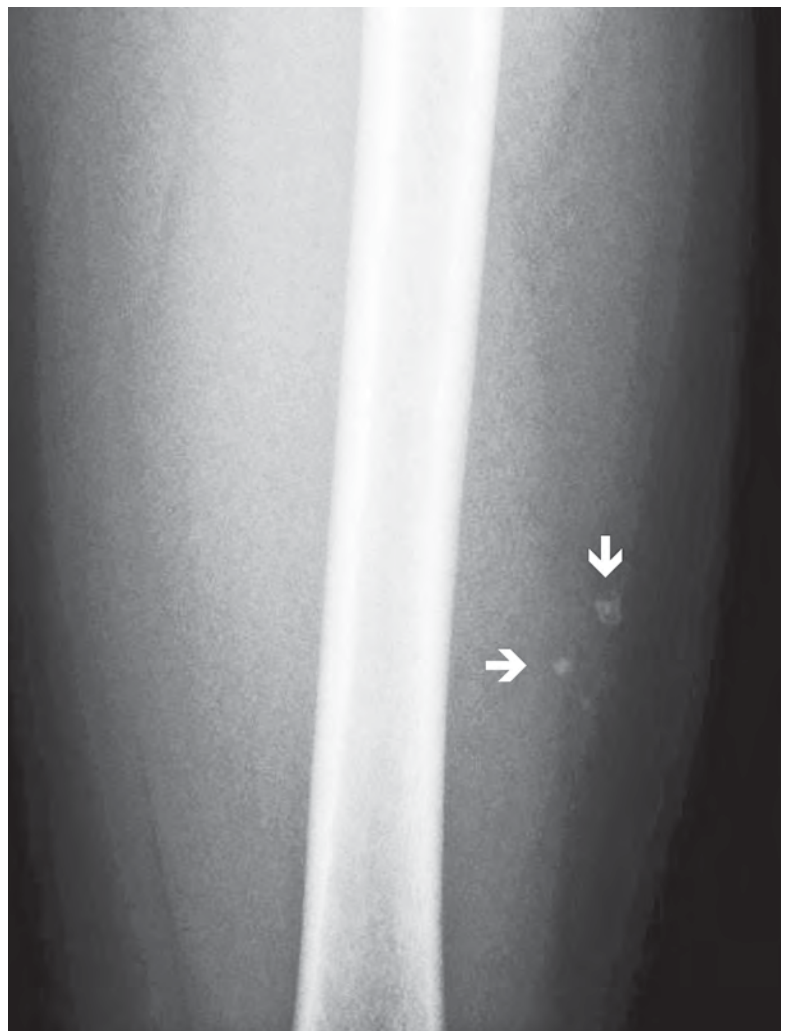
Case Summary

A child presented with left lateral thigh pain. The patient described the pain as progressing in severity and frequency for 17 months and alleviated with increased use of nonsteroidal anti-inflammatory medications.

Image Findings

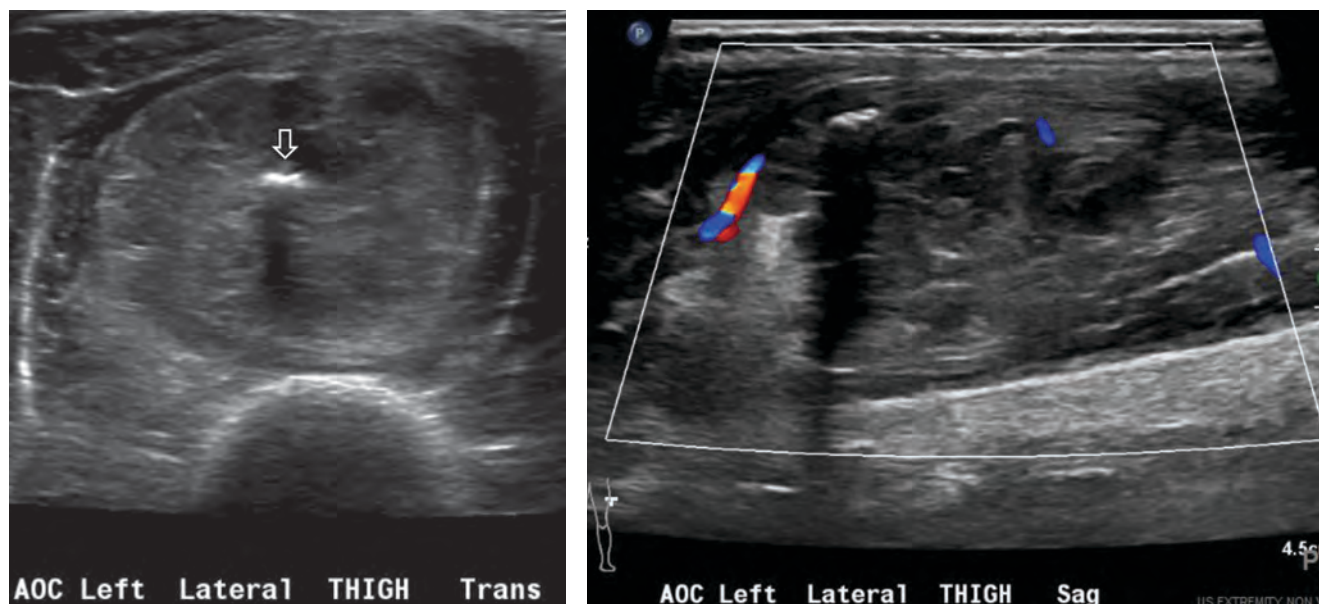
A radiograph of the left femur showed a cluster of small calcifications within the lateral soft tissues typical of phleboliths (Figure 1). Focused grayscale and color Doppler ultrasound (US) in the region of the soft tissue calcifications showed a $4.6 \times 2.2 \times 2.9$ cm, heterogeneous, soft-tissue mass with an echogenic focus with posterior acoustic shadowing and internal blood flow (Figure 2). For further evaluation, left lower-extremity MR imaging was recommended. The MRI revealed a lobulated, complex mass within the vastus intermedius muscle with heterogeneous signal and contrast enhancement with nonenhancing

Figure 1. A radiograph of the left femur shows a small cluster of rounded calcifications (arrows) about the lateral soft tissues, typical of phleboliths.



Affiliations: University of Arizona College of Medicine-Phoenix (Mr Nguyen); Phoenix Children's Hospital, Phoenix, AZ (Drs R Towbin, Schaefer, Aria); Cincinnati Children's Hospital (Dr A Towbin).

Figure 2. (A) Grayscale and color Doppler ultrasound of the left thigh show a $4.6 \times 2.2 \times 2.9$ cm, heterogeneous, soft-tissue mass with a single echogenic focus with associated shadowing (arrow). (B) Color Doppler interrogation shows mild internal blood flow.



foci, indicative of the phleboliths (Figure 3). An ultrasound-guided core-needle biopsy was performed; it confirmed diagnosis of a partially thrombosed venous malformation. The lesion was treated with sclerotherapy using absolute ethanol as the sclerosing agent.

Diagnosis

Congenital venous malformation. The differential diagnosis includes other slow-flow vascular malformations, specifically microcystic and macrocystic lymphatic malformations.

Discussion

The International Society for the Study of Vascular Anomalies classification of vascular anomalies categorizes vascular malformations according to the prominent abnormal vessel type. These types include the following: venous malformation (VM), lymphatic malformation (LM), capillary malformation (CM),

arteriovenous malformation (AVM), and arteriovenous fistulae (AVF).¹

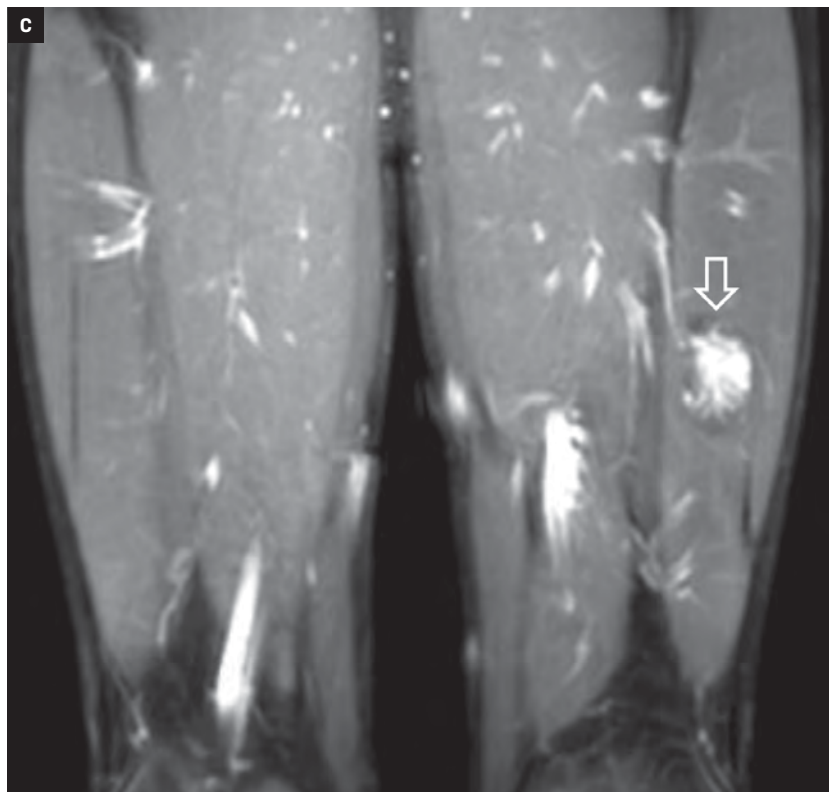
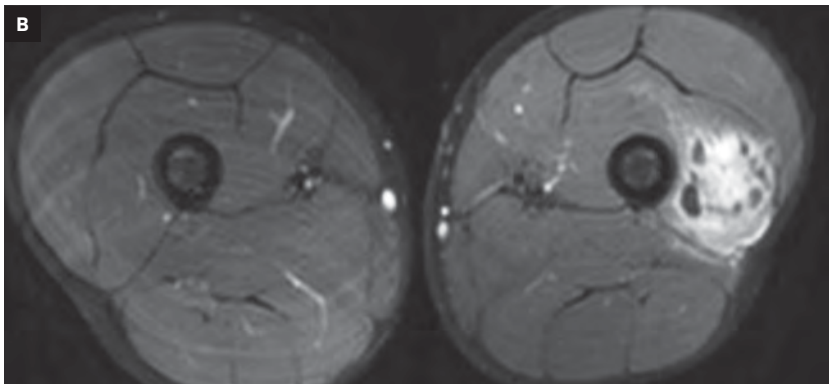
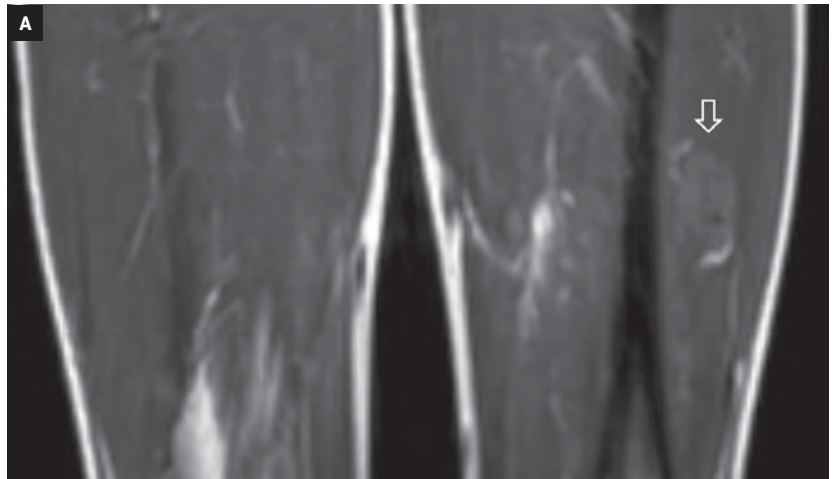
Venous malformations are the most common type of congenital vascular malformation; they have an incidence of about 1-2 per 10,000 and a prevalence of 1%. A VM is congenital, composed of abnormally formed veins that assume abnormal morphologies. The venous walls are abnormally thin with little smooth muscle, predisposing the vessel to dilatation.² Patients can have one or more VMs. Importantly, like all vascular malformations, VMs do not spontaneously resolve and they may recur. Clinically, VMs usually present at birth and grow proportionate to the patient's body size. However, some VMs are not evident until later in life especially those that are deep in the body. VMs are usually not painful, although some patients experience achy discomfort, especially later in the day, resulting from stasis of blood and venous engorgement or VM partial thrombosis. A significant increase in pain and swelling

can occur owing to an increase in mass effect or local hemorrhage. When VMs are superficial, they appear bluish, are compressible, and expand following compression release (in contrast to lymphatic malformations).

VMs may be familial in 1-2% of cases and are cutaneomucosal in distribution. Familial VMs are associated with a mutation of the protein receptor tyrosine kinase (TIE-2 gene) mapped to the 9p21-22 gene. VM subtypes occur in about 10% of individuals diagnosed with a VM. The clinical features and bodily distribution vary with specific subtype. Subtypes include:

- Glomuvenous malformations (GVM). GVMs occur sporadically or can be transmitted in an autosomal dominant fashion. The lesions appear as non-compressible, hyperkeratotic dark blue lesions, most often distributed superficially. Glomus cells are smooth muscle cells thought to regulate blood flow. In GVMs, these cells are abnormal and

Figure 3. (A) Coronal T1 image reveals a lobulated, complex mass (arrow) within the left vastus intermedius muscle with heterogenous hyperintense signal. (B) Axial and (C) Coronal post-contrast T1-fat sat images show heterogeneous enhancement of the VM (arrow) within the left vastus intermedius muscle.



may form multiple rows within the vascular space. GVMs may be solitary or multiple (10% of cases). The solitary type is often more painful, a feature that can differentiate it from the more common congenital VM. GVMs are congenital in at least 65% of patients due to a mutation in the glomulin gene (1p21).

- Blue Rubber Blue Nevus Syndrome lesions. (BRBN)/Bean Syndrome is a sporadic disorder characterized by multiple small, dark blue, rubbery lesions most often distributed on the skin and in the musculoskeletal and gastrointestinal systems. Histologically, these lesions have deficient smooth muscle cells and dysplastic venous channels.
- Maffucci syndrome lesions. Maffucci syndrome is a sporadic genetic disorder characterized by multiple enchondromas and spindle cell hemangiomas. The spindle cell hemangiomas are most often found asymmetrically on palms, soles, and extremities.

Long-term effects may include malignant degeneration of the enchondromas to chondrosarcomas and disfigurement resulting from the bone and vascular lesions.

- **Cerebral Cavernous Malformation (CCM).** CCM is a familial disorder associated with multiple VMs in the brain that often expand and bleed. About 10% of these patients also develop VMs of the skin. The CCMs are characterized histologically by clusters of hyalinized capillaries surrounded by gliosis and hemosiderin deposition. CCMs are most often found in the supratentorial brain and can be associated with developmental venous anomalies. MRI signal will vary depending on the presence and age of blood products.

Imaging is not often necessary to diagnose cutaneous VMs, but it is essential for evaluating deep lesions. However, diagnostic imaging and treatment planning are required when localized VMs present with pain, swelling, neurologic symptoms, or other forms of disfigurement and functional impairment or planning for image-guided sclerotherapy. Radiographs occasionally may be useful in diagnosing deep VMs if phleboliths or dystrophic calcifications are identified. Bony changes may be found in up to a third of patients with VMs.³ The presence of phleboliths can distinguish VMs from other types of vascular malformations; eg, lymphatic malformations do not have phleboliths. US and MRI are key to the diagnosis and differentiation of vascular malformations. Although CT may be more sensitive in identifying phleboliths, the modality is no longer used as a primary diagnostic modality owing to its ionizing radiation and lower

(compared to MRI) soft-tissue resolution/differentiation.²

Doppler US is often useful for initial examination of a suspected vascular malformation. The typical diagnostic features of VMs include a compressible, soft-tissue mass made up of venous channels and a relatively small amount of soft tissue. VM lesions are hypoechoic or anechoic masses with slow intralesional blood flow. During contrast-enhanced US, enhancement may be seen in the venous phase.

MRI with gadolinium contrast enhancement is the gold standard for diagnosis. VMs typically appear as septated, lobular masses with high-intensity signal on T2 or STIR imaging and intermediate-low signal on T1 images; there is also a lack of flow voids. Importantly, no abnormal arterial flow or arterial enlargement is present. Typically, VMs do not exert mass effect on adjacent structures. Diffuse enhancement on postcontrast imaging is also indicative of VMs. Phleboliths are identified by low intensity foci on all pulse sequences.⁴

Treatment options include medical management, surgery, laser therapy, and sclerotherapy. Medical management includes low-dose NSAIDs for pain control and, in some cases, low molecular weight heparin to prevent localized coagulopathy.⁵ Compression stockings can be used for swelling in the extremities. However, these medical therapies do not treat the underlying pathology.

Image guided sclerotherapy is today's first-line treatment for VMs.⁶ The goal is to cause intimal injury to endothelial cells that leads to localized, intralesional thromboses and ultimate fibrosis so that no significant blood flow occurs in the VM. Multiple sclerotherapy sessions are often needed to sig-

nificantly improve the lesion; US is used to guide sclerotherapy and to monitor treatment progression.

The choice of treatment agent is often related to the preference and experience of the treating physician. Ethanol is one of the most common and effective sclerosing agents. Alternative agents include sodium tetradecyl sulfate (STS) and polidocanol, which are less effective in our experience. Bleomycin is a newer, effective option with fewer complications than absolute ethanol, especially with respect to skin necrosis. However, the therapeutic effect takes considerably longer and requires longer intervals between follow-up visits. Post-procedurally, patients are managed with analgesics and anti-inflammatory drugs.

The expected side effects of sclerotherapy include edema and inflammation; the VM and surrounding tissue commonly appear swollen and painful to touch post-therapy. Major complication rates vary with sclerosing agent.⁷ A retrospective study of outcomes in 153 patients with VMs reported a grade 3 (requiring plastic surgery intervention) complication rate of 2% and a grade 4 (permanent scar at injection site) complication rate of 7%.⁸ The most common serious complications include disseminated intravascular coagulation, nerve injury, infection, and skin necrosis. On rare occasions, local swelling can cause a compartment syndrome. However, complications such as pulmonary hypertension, pulmonary embolism, arrhythmia, and hemoglobinuria can occur if the sclerosing agent enters the systemic circulation. Because of these risks, some practices routinely obtain blood alcohol levels to monitor the patient post-sclerotherapy and use a weight-based dosage of ethanol.

Mean time to potential recurrence is 7-37 months.⁹ The literature consistently reports clinical improvement among most patients after sclerotherapy, although many report previous treatment for VMs. Recovery is assessed based on a combination of patient's subjective symptoms and reduction in lesion size.

Conclusion

Venous malformations are the most common type of congenital vascular malformation and are usually not related to familial or syndromes causes. Most VMs are diagnosed clinically with imaging. The primary therapy today is minimally invasive, image-guided sclerotherapy.

References

- 1) Monroe EJ. Brief description of ISSVA classification for radiologists. *Tech Vasc Interv Radiol* 2019; 22:100628.
- 2) Steiner JE, Drolet BA. Classification of vascular anomalies: an update. *Semin Intervent Radiol*. 2017; 34:225-232.
- 3) Behraves S, Yakes W, Gupta N, et al. Venous malformations: clinical diagnosis and treatment. *Cardiovasc Diagn Ther*. 2016;6:557-569.
- 4) Flors L, Leiva-Salinas C, Maged IM, et al. MR imaging of soft-tissue vascular malformations: diagnosis, classification, and therapy follow-up. *Radiographics*. 2011;31:1321-1331.
- 5) Hage AN, Chick JFB, Srinivasa RN, et al. Treatment of venous malformations: the data, where we are now, and how it is done. *Tech Vasc Interv Radiol*. 2018; 21:45-54.
- 6) Pappas DC Jr., Persky MS, Berenstein A. Evaluation and treatment of head and neck venous vascular malformations. *Ear Nose Throat J*. 1998; 77(11): 914-16, 918-922.
- 7) Ali S, Mitchell SE. Outcomes of venous malformation sclerotherapy: a review of study methodology and long-term results. *Semin Intervent Radiol*. 2017; 34:288-293.
- 8) Gorman J, Zbarsky SJ, Courtemanche RJM, Arneja JS, Heran MKS, Courtemanche DJ. Image guided sclerotherapy for the treatment of venous malformations. *CVIR endovascular* 2018; 1:2. doi:10.1186/s42155-018-0009-1
- 9) Khaitovich B, Kalderon E, Komisar O, Eifer M, Raskin D, Rimón U. Venous malformations sclerotherapy: outcomes, patient satisfaction and predictors of treatment success. *Cardiovasc Intervent Radiol*. 2019;42:1695-1701.

IMPORTANT SAFETY INFORMATION³

WARNING: NEPHROGENIC SYSTEMIC FIBROSIS (NSF)

Gadolinium-based contrast agents (GBCAs) increase the risk for NSF among patients with impaired elimination of the drugs. Avoid use of GBCAs in these patients unless the diagnostic information is essential and not available with non-contrast MRI or other modalities. NSF may result in fatal or debilitating fibrosis affecting the skin, muscle and internal organs.

- The risk for NSF appears highest among patients with:
 - Chronic, severe kidney disease (GFR < 30 mL/min/1.73m²), or
 - Acute kidney injury.
- Screen patients for acute kidney injury and other conditions that may reduce renal function. For patients at risk for chronically reduced renal function (e.g. age > 60 years, hypertension, diabetes), estimate the glomerular filtration rate (GFR) through laboratory testing.
- For patients at highest risk for NSF, do not exceed the recommended DOTAREM dose and allow a sufficient period of time for elimination of the drug from the body prior to any re-administration.

INDICATIONS AND USAGE

DOTAREM[®] (gadoterate meglumine) injection is a prescription gadolinium-based contrast agent indicated for intravenous use with magnetic resonance imaging (MRI) in brain (intracranial), spine and associated tissues in adult and pediatric patients (including term neonates) to detect and visualize areas with disruption of the blood brain barrier (BBB) and/or abnormal vascularity.

CONTRAINDICATIONS

History of clinically important hypersensitivity reactions to DOTAREM.

WARNINGS AND PRECAUTIONS

- Hypersensitivity Reactions: Anaphylactic and anaphylactoid reactions have been reported with DOTAREM, involving cardiovascular, respiratory, and/or cutaneous manifestations. Some patients experienced circulatory collapse and died. In most cases, initial symptoms occurred within minutes of DOTAREM administration and resolved with prompt emergency treatment.
- Before DOTAREM administration, assess all patients for any history of a reaction to contrast media, bronchial asthma and/or allergic disorders. These patients may have an increased risk for a hypersensitivity reaction to DOTAREM.
- Administer DOTAREM only in situations where trained personnel and therapies are promptly available for the treatment of hypersensitivity reactions, including personnel trained in resuscitation.
- Gadolinium Retention: Gadolinium is retained for months or years in several organs. The highest concentrations have been identified in the bone, followed by brain, skin, kidney, liver and spleen. The duration of retention also varies by tissue, and is longest in bone. Linear GBCAs cause more retention than macrocyclic GBCAs.
- Consequences of gadolinium retention in the brain have not been established. Adverse events involving multiple organ systems have been reported in patients with normal renal function without an established causal link to gadolinium retention.
- Acute Kidney Injury: In patients with chronically reduced renal function, acute kidney injury requiring dialysis has occurred with the use of GBCAs. The risk of acute kidney injury may increase with increasing dose of the contrast agent; administer the lowest dose necessary for adequate imaging.
- Extravasation and Injection Site Reactions: Ensure catheter and venous patency before the injection of DOTAREM. Extravasation into tissues during DOTAREM administration may result in tissue irritation.

ADVERSE REACTIONS

- The most common adverse reactions associated with DOTAREM in clinical trials were nausea, headache, injection site pain, injection site coldness and rash.
- Serious adverse reactions in the Postmarketing experience have been reported with DOTAREM. These serious adverse reactions include but are not limited to: arrhythmia, cardiac arrest, respiratory arrest, pharyngeal edema, laryngospasm, bronchospasm, coma and convulsion.

USE IN SPECIFIC POPULATIONS

- Pregnancy: GBCAs cross the human placenta and result in fetal exposure and gadolinium retention. Use only if imaging is essential during pregnancy and cannot be delayed.
- Lactation: There are no data on the presence of gadoterate in human milk, the effects on the breastfed infant, or the effects on milk production. However, published lactation data on other GBCAs indicate that 0.01 to 0.04% of the maternal gadolinium dose is present in breast milk.
- Pediatric Use: The safety and efficacy of DOTAREM at a single dose of 0.1 mmol/kg has been established in pediatric patients from birth (term neonates ≥ 37 weeks gestational age) to 17 years of age based on clinical data. The safety of DOTAREM has not been established in preterm neonates. No cases of NSF associated with DOTAREM or any other GBCA have been identified in pediatric patients age 6 years and younger.

You are encouraged to report negative side effects of prescription drugs to the FDA. Visit www.fda.gov/medwatch or call 1-800-FDA-1088.

Please see the full Prescribing Information, including Boxed Warning and the patient Medication Guide, for additional important safety information.

References: 1. Port M et al. Efficiency, thermodynamic and kinetic stability of marketed gadolinium chelates and their possible clinical consequences: a critical review. *Biometals*. 2008;21:469-90. 2. Frenzel T et al. Stability of gadolinium-based magnetic resonance imaging contrast agents in human serum at 37°C. *Invest Radiol*. 2008;43:817-828. 3. Dotarem [package insert]. Princeton, NJ: Guerbet LLC; Oct 2019. 4. De-Hua, Chang, and Pracros Jean-Pierre. "Safety of Gadoterate Meglumine in over 1600 Children Included in the Prospective Observational SECURE Study." *Acta Radiologica*, 2019. 5. Mithal LB, Patel PS, Mithal D, Palac HL, Rozenfeld MN. Use of gadolinium-based magnetic resonance imaging contrast agents and awareness of brain gadolinium deposition among pediatric providers in North America. *Pediatr Radiol*. 2017 Mar10;doi: 10.1007/s00247-017-3810-4. [Epub ahead of print] 6. Radbruch A et al. Gadolinium retention in the dentate nucleus and globus pallidus is dependent on the class of contrast agent. *Radiology*. 2015 Jun;275(3):783-91. 7. Radbruch A et al. Intraindividual analysis of signal intensity changes in the dentate nucleus after consecutive serial applications of linear and macrocyclic gadolinium-based contrast agents. *Invest Radiol*. 2016 Nov;51(11):683- 690. 8. Eisele P et al. Lack of increased signal intensity in the dentate nucleus after repeated administration of a macrocyclic contrast agent in multiple sclerosis: An observational study. *Medicine (Baltimore)*. 2016 Sep;95(39):e4624. 9. Radbruch A et al. Pediatric brain: no increased signal intensity in the dentate nucleus on unenhanced T1-weighted MR images after consecutive exposure to a macrocyclic gadolinium-based contrast agent. *Radiology*. 2017 Mar 8;162980. [Epub ahead of print]. 10. Tibussek D et al. Gadolinium Brain Deposition after Macrocyclic Gadolinium Administration: A Pediatric Case-Control Study. *Radiology*. 2017 161151 [Epub ahead of print].

DOTAREM[®] is a registered trademark of Guerbet and is available by prescription only.

*Dotarem was launched globally in 1989 and approved by the FDA for use in the US in 2013

DOTAREM[®]

(gadoterate meglumine) Injection

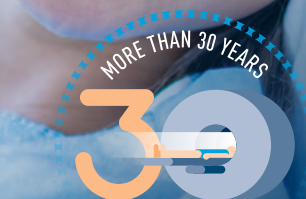
A Stable MRI Contrast Solution Approved for Children

The safety and efficacy of Dotarem have been established in pediatric patients from birth (term neonates \geq 37 weeks gestational age) to 17 years of age.¹⁻³

- Available in a wide variety of dosing options, including 5mL vials
- In a pediatric study of 1,568 patients, image quality was rated either good or very good by radiologists in 98.4% of cases when using Dotarem⁴
- Many pediatric hospitals have or plan to switch to Dotarem, a stable macrocyclic GBCA⁵
- The only imaging contrast with a macrocyclic and ionic structure for high thermodynamic and kinetic stability^{1,2}
- Following repeated administration, no visible T1 signal intensity detected on non-contrast images within the brain⁶⁻¹⁰

Guerbet | 

COMMITTED



DOTAREM[®]
(gadoterate meglumine) Injection

1-877-729-6679 | Dotarem-us.com

Telangiectatic Osteosarcoma

Colby S Nielsen; Richard B Towbin, MD; Carrie M Schaefer, MD; Alexander J Towbin, MD; David J Aria, MD

Case Summary

An adolescent presented with dull, achy pain, swelling, and reduced range of motion of their left shoulder.

Imaging Findings

Radiographs of the shoulder demonstrated an expansile, transcortical, lucent lesion that involved the epiphysis, metaphysis, and much of the proximal diaphysis of the left humerus (Figure 1). The tumor had aggressive features with a wide zone of transition, and periosteal new bone formation, creating a Codman triangle, the triangular area of new subperiosteal bone that is created when a lesion, often a tumor, raises the periosteum away from the bone. Magnetic resonance imaging (MRI) of the left humerus showed an expansile, T2 hyperintense lesion with multiple septations and internal fluid-fluid levels (Figure 2). Ultrasound-guided percutaneous needle biopsy (Figure 3) was performed for definitive diagnosis.

Diagnosis

Telangiectatic osteosarcoma (TO). Differential diagnosis includes aneurysmal bone cyst.

Aneurysmal bone cysts can either represent a primary lesion or can occur as a secondary lesion associated with other tumors such as osteosarcoma, giant cell tumor, and chondroblastoma.

Discussion

Telangiectatic osteosarcoma (TO) is an uncommon variant of osteosarcoma, occurring in 4% of osteosarcoma cases.¹ Patients with TO present with pain, a soft-tissue mass, and/or a pathological fracture.² Telangiectatic osteosarcoma occurs two times more frequently in males and the average age at diagnosis varies between 15 and 20 years.¹ Over 65% of TOs develop in the metaphysis of the femur or the humerus, with the distal femur being the most common location (41.6%). Other reported sites of tumor development include the mid-femur, mid-humerus, mid-tibia, pelvis, fibula, skull, and ribs. Like that of other osteosarcomas, TO diagnosis is made by a combination of skeletal radiographs and computed tomography and/or MRI

and confirmed by bone biopsy. TO and conventional osteosarcoma are compared in Table 1.

On imaging, radiographs show a lucent lesion with a destructive growth pattern involving medullary and cortical bone. TO shows little to no periosteal new bone formation, except for isolated regions near the periphery of the tumor and within the septa, where atypical stromal cells may be localized.¹ This contrasts with traditional osteosarcoma, in which aggressive periosteal new bone formation is often present.⁴ A Codman triangle is commonly seen in TO.¹

On MRI, T1 images frequently show high-signal intensity regions due to methemoglobin within hemorrhagic spaces. T2 images demonstrate multiple fluid-fluid levels owing to fluids of different densities settling within cystic cavities of the lesion.

Aneurysmal bone cysts are the most common lesions with multiple fluid-fluid levels on imaging. It can be difficult to distinguish an aneurysmal bone cyst from a TO. Other MR imaging features can help to distinguish the two entities, as a TO may have thickened and nodular internal septations owing to the viable sarcomatous cells. A soft-tissue mass may also be present.¹

Affiliations: University of Arizona—Phoenix (Mr Nielsen); Phoenix Children's Hospital, Phoenix, Arizona (Drs R Towbin, Schaefer, Aria); Cincinnati Children's Hospital, Cincinnati, Ohio (Dr A Towbin).

Figure 1. Radiographs of the left shoulder show an expansile, lucent lesion of the proximal left humerus. There is a wide zone of transition, thinning of the cortex, and a heterogeneous internal matrix with amorphous septations. A Codman triangle of periosteal new bone (arrow) is present along the inferolateral portion of the tumor.

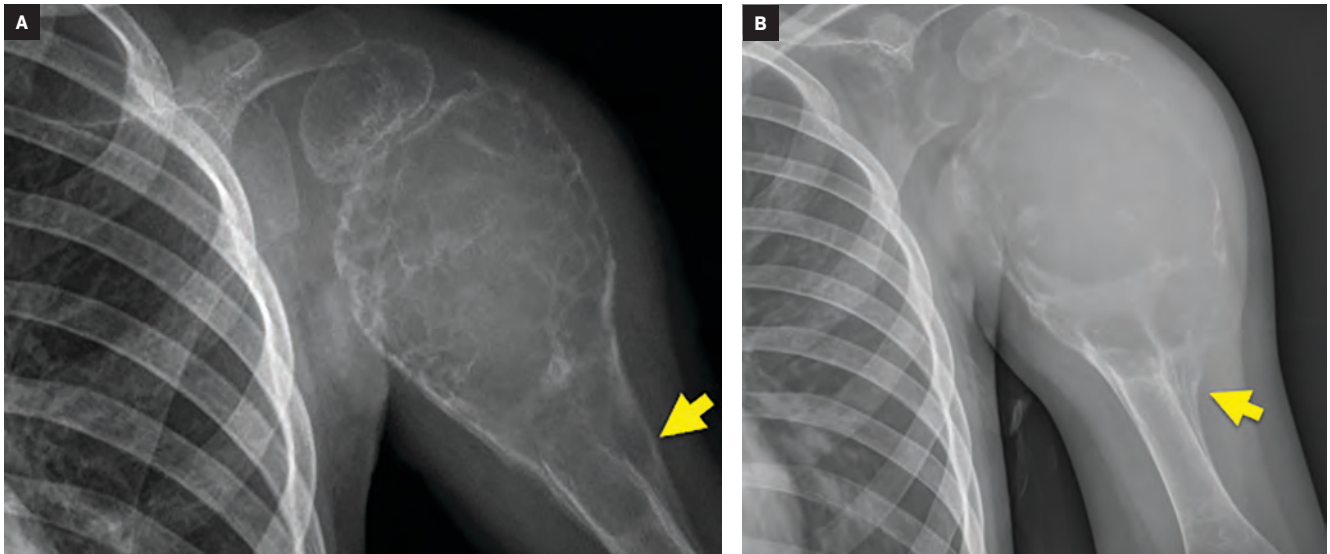


TABLE 1. COMPARISON OF TELANGIECTATIC OSTEOSARCOMA AND OSTEOGENIC SARCOMA

	Telangiectatic Osteosarcoma	Osteosarcoma
Clinical presentation	<ul style="list-style-type: none"> Local pain² Soft-tissue mass² Rarely, pathological fracture² 	<ul style="list-style-type: none"> Local pain² Soft-tissue mass² Rarely, pathological fracture²
Average age at presentation (yrs)	15-20 ¹	15 ³
Epidemiological characteristics	Males 2x more likely ¹	Males 1.22x more likely ³
Anatomic location	Most commonly metaphyseal portions of long bones ¹	Most commonly metaphyseal portions of long bones ^{1,3}
Imaging findings	<ul style="list-style-type: none"> Codman triangle^{1,2} Wide zone of transition^{1,2} Cortical invasion^{1,2} Lytic lesion, little mineralization^{1,2} Fluid-filled cavities with methemoglobin^{1,2} 	<ul style="list-style-type: none"> Codman triangle³ Wide zone of transition³ Cortical invasion³ Lucent and sclerotic features³ Speculated periosteal bone formation ("sunburst appearance")³ Mineralized soft-tissue mass³
Overall survival	67% ¹	58.3%-69 ^{1,9}
5-year event-free survival	58% ¹	44.3% ¹

The histologic findings of TO are similar to those of an aneurysmal bone cyst.¹ Both lesions are composed mostly of necrotic tissue and clotted blood with thin septa of atypical stromal cells throughout. While identification of malignant cells may be difficult, it is enough to rule out diagnosis of a primary aneurysmal bone cyst. TO may be categorized histologically as low-grade (mild to moderate nuclear

atypia and few mitoses) or high-grade (anaplastic cells with high mitotic activity).¹

Patients with TO are treated with a combination of neoadjuvant chemotherapy and surgical resection. However, TO appears to be more sensitive to neoadjuvant chemotherapy than conventional osteosarcoma, and some patients can be cured with neoadjuvant therapy alone.⁶

The patterns of recurrence and metastasis in TO are similar to those of conventional osteosarcoma. In a review of 87 patients with TO at 10 years of follow-up, Angellini et al found local recurrence in 11% of patients, lung metastases in 25%, and bone metastases in 3.4%.⁷ In conventional osteosarcoma, metastases occur in 25-30% of patients, with 85% in the lungs and 10% in the bone.⁸

Figure 2. Axial T2 MRI with fat saturation shows the large, expansile mass of the proximal left humerus containing numerous fluid-fluid levels and fine internal septations..



While early reports of TO describe a more aggressive tumor with poorer outcomes than conventional osteosarcoma, more recent literature since the advent of neoadjuvant chemotherapy indicates that TO may now have a similar prognosis.³ The current five-year survival rate of TO is 60-80%, which is like that of conventional osteosarcoma, which has a five-year survival rate of 69%.⁹

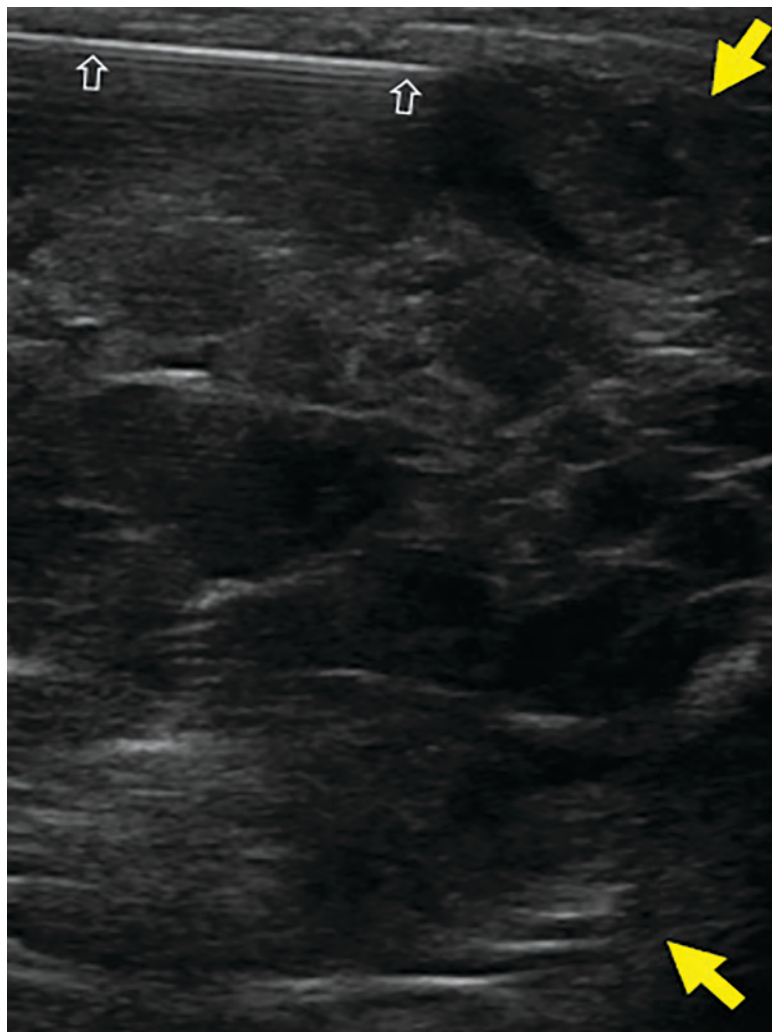
Conclusion

Telangiectatic osteosarcoma represents a rare, malignant bone tumor, typically presenting between the ages of 15 and 20 years. TO often presents as a tender to touch, irregular mass or occasionally a pathological fracture. Notable in the differential diagnosis is aneurysmal bone cyst, from which it is important to differentiate, given that prognosis and treatment differ drastically between each. Thickening and nodularity of septa and the periphery of the lesion as seen on MRI, along with malignant, atypical stromal cells, distinguishes TO.

References

1) Sangle NA, Layfield LJ. Telangiectatic osteosarcoma. *Arch Pathol Lab Med.* 2012 May;136(5):572-6. doi: 10.5858/arpa.2011-0204-RS. PMID: 22540307.

Figure 3. Ultrasound image obtained during percutaneous needle biopsy shows the needle (open arrows) at the superficial margin of the multiloculated mass (bounded by yellow arrows).



2) Limaïem F, Kuhn J, Khaddour K. Cancer, Telangiectatic Osteosarcoma. In: StatPearls. Treasure Island (FL): StatPearls Publishing; 2019. <http://www.ncbi.nlm.nih.gov/books/NBK537309/>. Accessed January 14, 2020.

3) Liu J, Liu S, Wang J, et al. Telangiectatic osteosarcoma: a review of literature. *Onco Targets Ther.* 2013;6:593-602. doi:10.2147/OTT.S41351

4) Moore DD, Luu HH. Osteosarcoma. In: Peabody TD, Attar S, eds. *Orthopaedic Oncology: Primary and Metastatic Tumors of the Skeletal System. Cancer Treatment and Research.* Cham: Springer International Publishing; 2014:65-92. doi:10.1007/978-3-319-07323-1_4

5) Keenan S, Bui-Mansfield LT. Musculoskeletal lesions with fluid-fluid level: A pictorial essay. *J Comp Assist Tomog.* 2006;30(3):517-524.

6) Carrasco CH, Charnsangavej C, Richli WR, et al. Osteosarcoma: interventional radiology

in diagnosis and management. *Semin Roentgenol.* 1989;24(3):193-200. doi:10.1016/0037-198X(89)90014-X

7) Angelini A, Mavrogenis AF, Trovarelli G, et al. Telangiectatic osteosarcoma: a review of 87 cases. *J Cancer Res Clin Oncol.* 2016;142(10):2197-2207. doi:10.1007/s00432-016-2210-8

8) Poletajew S, Fus L, Wasiutyński A. Current concepts on pathogenesis and biology of metastatic osteosarcoma tumors. *J Orthop Traumatol Rehab.* 2011;13(6):537-545. doi:10.5604/15093492.971038

9) Osteosarcoma - Childhood and Adolescence: Statistics. Cancer.net. <https://www.cancer.net/cancer-types/osteosarcoma-childhood-and-adolescence/statistics#:~:text=The%20overall%205%2Dyear%20survival,of%20all%20ages%20is%2077%25.> Accessed July 13, 2020.

Middle Aortic Syndrome

Kenneth Zurcher, MD; Richard B Towbin, MD; Carrie M Schaefer; Scott A Jorgensen, MD; Alexander J Towbin, MD

Case Summary

An adolescent presented with chronic, severe hypertension (systolic >200 mmHg) not controlled by antihypertensive medications. A cardiology workup detected left ventricular hypertrophy.

Imaging Findings

An axial CT angiogram (CTA, Figure 1) demonstrated a narrowed segment of the thoracoabdominal aorta measuring 3-4 mm in greatest diameter extending above the level of the celiac trunk and superior mesenteric arteries. Numerous collateral vessels were present in the anterior thoracic and abdominal wall.

Diagnosis

Middle aortic syndrome. Differential diagnosis includes primary hypertension resulting from renovascular hypertension, chronic renal disease, polycystic kidney disease, coarctation of the aorta,

adrenal tumors, hyperthyroidism, medication-induced vessel scarring, and Kawasaki disease. Differential also includes aortic narrowing resulting from neurofibromatosis type 1, tuberous sclerosis, Williams syndrome, Alagille syndrome, and Takayasu arteritis.

Discussion

Middle aortic syndrome (MAS) is a rare vascular disorder that results in segmental narrowing of the abdominal or distal descending thoracic aorta. The stenosis is often accompanied by osteal stenosis of the aortic branches, especially the proximal renal and visceral arteries. The narrowing can be congenital or acquired. Fewer than 700 cases have been reported to date,¹ with MAS constituting approximately 0.5-2% of all cases of aortic stenosis in children and young adults.²

Typically presenting in the pediatric population, MAS can result in significant morbidity secondary to stenosis of the aorta and its associated abdominal visceral branches. In a recent systematic review of 630 patients <18 years of age in 184 publications, the mean age at presentation was estimated to be 9.1 +/- 5 years. Children often presented with severe upper extremity or reno-

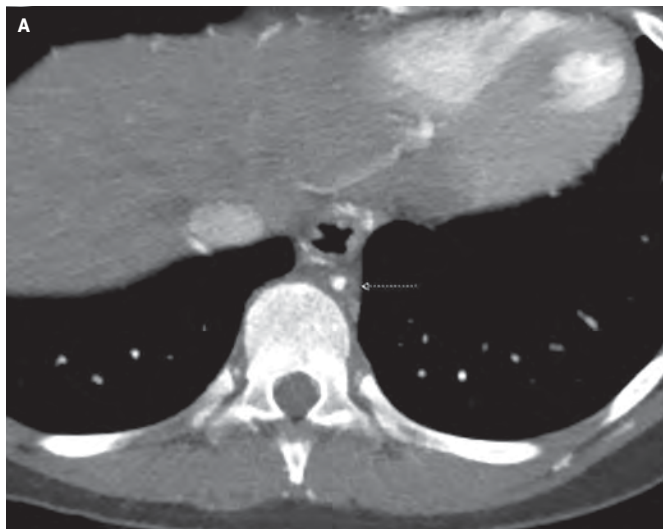
vascular hypertension (>87%). Other presentations included abdominal bruit (23%), headache (13%), lower-extremity claudication (10%) and absent femoral pulses (7%).¹ Left untreated, patients can suffer from vascular sequelae such as left ventricular hypertrophy (30%), congestive heart failure (9%), cardiomegaly (7%), neurologic deficits (7%) or decreased renal function (6%).

The etiology of MAS is not well understood; approximately 64% of cases are idiopathic. Congenital MAS is caused by a developmental anomaly in the fusion and maturation of the paired embryonic dorsal aortas and typically is diagnosed early in life. Acquired causes of MAS include neurofibromatosis type 1, Williams syndrome, Alagille syndrome, fibromuscular dysplasia, retroperitoneal fibrosis, mucopolysaccharidosis, and arteritides such as Takayasu arteritis.³⁻⁷

While catheter angiography was previously considered as the gold standard for diagnosing idiopathic MAS,⁸ the condition now can be effectively diagnosed with computed tomography angiography (CTA) or magnetic resonance angiography (MRA). No guidelines exist on the optimal workup for MAS, but detection of aortic stenosis by ultrasound has also been described, with pa-

Affiliations: Mayo Clinic, Scottsdale, AZ (Dr Zurcher); Phoenix Children's Hospital, Phoenix, AZ (Drs R Towbin, Schaefer, Jorgensen); Cincinnati Children's Hospital, Cincinnati, OH (Dr A Towbin)

Figure 1. (A) Axial CTA image of the chest demonstrates a narrowed thoracoabdominal aorta (arrow) measuring 3-4mm in greatest diameter. (B) Sagittal CTA MIP image shows narrowing of the thoracoabdominal aorta (arrow) with severe stenosis of the celiac axis (curved arrow). (C) 3D reformatted image shows aortic narrowing (arrow) to the level of the celiac and superior mesenteric arteries. (D) 3D reformatted image shows marked collateralization of the internal thoracic arteries and the superior and inferior epigastric arteries.



tients often receiving a subsequent CTA or MRA to further delineate the involved vessels. In the aforementioned systematic review, segmental or diffuse narrowing of the abdominal aorta was noted in 97% of cases, with thoracic involvement in 3%, renal artery involvement in 66.2%, superior mesenteric artery involvement in 29.5%, and celiac axis involvement in 22.4%.¹

A multidisciplinary approach is critical to managing patients with MAS. Treatment strategies vary depending upon the nature of the aortic stenosis, the extent of visceral involvement, and the presence of secondary co-morbidities. Medical management has been utilized in uncomplicated cases, with varying results. In addition to medical management, patients can be treated with endovascular interventions such as angioplasty with or without stent placement or surgery.

Surgical options depend on location of the stenosis and the affected vessels. Potential options include aorto-aortic bypass,

reconstruction patch graft, or renal auto-transplantation. Indications for surgical or endovascular intervention include high risk of renal failure, refractory hypertension, claudication, and intestinal ischemia.⁸ Blood pressure control following endovascular intervention with and without subsequent medication is reported to be 36% and 18%, respectively. After surgical intervention, control with and without subsequent medication is reported to be 55% and 25%, respectively.¹

Conclusion

MAS may be congenital or acquired. Medical therapy may control blood pressure but does not treat the underlying aortic stenosis. Currently, no therapeutic approach is curative. Surgery is the primary treatment for congenital causes of MAS, with balloon angioplasty or cutting balloon angioplasty a consideration in other select instances.

References

- 1) Rumman RK, Nickel C, Matsuda-Abedini M, et al. Disease beyond the arch: a systematic review of middle aortic syndrome in childhood. *Am J Hypertens*. 2015;28(7):833-846. DOI: 10.1093/ajh/hpu296
- 2) Cohen JR, Birnbaum E. Coarctation of the abdominal aorta. *J Vasc Surg*. 1988; 8:160-164.
- 3) Connolly JE, Wilson SE, Lawrence PL, Fujitani RM. Middle aortic syndrome: distal thoracic and abdominal coarctation, a disorder with multiple etiologies. *J Am Coll Surg*. 2002; 194:774-781.
- 4) Criado E, Izquierdo L, Luján S, Puras E, del Mar Espino M. Abdominal aortic coarctation, renovascular, hypertension, and neurofibromatosis. *Ann Vasc Surg*. 2002;16:363-367.
- 5) Raas-Rothschild A, Shteyer E, Lerer I, Nir A, Granot E, Rein AJ. Jagged1 gene mutation for abdominal coarctation of the aorta in Alagille syndrome. *Am J Med Genet*. 2002; 112:75-78.
- 6) Radford DJ, Pohlner PG. The middle aortic syndrome: an important feature of Williams' syndrome. *Cardiol Young*. 2000;10:597-602.
- 7) Taketani T, Miyata T, Morota T, Takamoto S. Surgical treatment of atypical aortic coarctation complicating Takayasu's arteritis-experience with 33 cases over 44 years. *J Vasc Surg*. 2005;41:597-601.
- 8) Sethna CB, Kaplan BS, Cahill AM, Velazquez OC, Meyers KE. Idiopathic mid-aortic syndrome in children. *Pediatr Nephrol*. 2008; 23:1135-1142. doi: 10.1007/s0067-008-0767-4

